

Origin of experimental order-disorder transition line curvature in the $\text{La}_{2-x}\text{Sr}_x\text{CuO}_4$ single crystal vortex system at low temperatures

著者	Miu L., Adachi T., Koike Y., Miu D., Diaz S., Chouteau G.
journal or publication title	Physical Review. B
volume	72
number	5
page range	052513
year	2005
URL	http://hdl.handle.net/10097/52941

doi: 10.1103/PhysRevB.72.052513

Origin of experimental order-disorder transition line curvature in the $\text{La}_{2-x}\text{Sr}_x\text{CuO}_4$ single crystal vortex system at low temperatures

L. Miu

National Institute of Materials Physics, Bucharest, MG-7, Romania

T. Adachi and Y. Koike

Department of Applied Physics, Tohoku University, 6-6-05 Aoba, Aramaki, Aoba-ku, Sendai 980-8579, Japan

D. Miu

National Institute of Laser, Plasma, and Radiation Physics, Bucharest, MG-6, Romania

S. Diaz and G. Chouteau

Grenoble High Magnetic Field Laboratory, B. P. 166, 38042 Grenoble, Cedex 9, France

(Received 22 December 2004; published 30 August 2005)

We investigated the dc magnetization curves of overdoped $\text{La}_{2-x}\text{Sr}_x\text{CuO}_4$ single crystals in the low-temperature T range, with the external magnetic field H oriented along the c axis. It was found that the onset field for the second magnetization peak, associated with the order-disorder transition in the vortex system, increases significantly with decreasing T in the low- T region, where the superconductor parameters are independent of T . The upward curvature of the order-disorder transition line determined in standard magnetization measurements at low T is explained by considering the reduction of the actual pinning energy due to the macroscopic currents induced in the sample. A simple energy balance equation for the dynamic conditions generated in the widely performed magnetization studies is proposed.

DOI: [10.1103/PhysRevB.72.052513](https://doi.org/10.1103/PhysRevB.72.052513)

PACS number(s): 74.25.Ha

The vortex phase diagram of disordered high-temperature superconductors (HTS') is dominated by an order-disorder transition in the vortex system,¹⁻⁴ accompanied by the appearance of a second peak on the dc magnetization curves.⁵⁻⁸ Significant progress for the understanding of the vortex phase diagram of HTS' in the presence of pinning has been made by considering the competition between the energy of thermal fluctuations, the pinning energy generated by the quenched disorder, E_{pin} , and the elastic energy of the vortex system, E_{el} .² The transition lines are approximately determined by matching any two of these energies. If the thermal energy is small compared with E_{el} and E_{pin} , when E_{pin} overcomes E_{el} one expects a quenched-disorder-driven transition between the quasi-ordered vortex solid at low H (the Bragg glass, stable against the dislocation formation^{9,10}) and a high-field-disordered vortex phase. In the disordered vortex phase there is a better accommodation of vortices to the pinning centers, and this transition manifests itself by the occurrence of the second magnetization peak (SMP). The transition field at low T should then roughly result² from the equality $E_{\text{el}}(T, H) = E_{\text{pin}}(T, H)$. As known, both E_{pin} and E_{el} depend on the superconductor parameters—the penetration depth, the coherence length, the pinning parameter, and the anisotropy factor γ . For T well below the critical temperature T_c , all the superconductor parameters are T independent,⁸ and, consequently, the transition field should be constant in T in the low- T domain (neglecting demagnetization effects), regardless of the variation of E_{el} and E_{pin} with H .

The transition field in disordered HTS' is associated with the field value H_{on} corresponding to the onset of the SMP. The T variation of the transition field observed for

$\text{La}_{2-x}\text{Sr}_x\text{CuO}_4$ single crystals in H perpendicular to the c axis (weak pinning) was discussed, over a large T interval, in terms of a unified order-disorder transition in the vortex system (when the transition is driven by both thermally and quenched-disorder-induced fluctuations),¹¹ based on the energy balance equation¹² $E_{\text{el}} = E_{\text{pin}} + T$. However, in the geometry with H parallel to the c axis, the static pinning energy E_{pin} is high, and the contribution of thermal energy at low T becomes negligible. Indeed, in the case of HTS' with significant quenched disorder, the resulting transition field for static conditions is nearly constant in the low- T domain.^{12,13} Alternatively, a three-step fitting procedure (based on different pinning mechanisms in three T regions) has been proposed to explain the nonmonotonic $H_{\text{on}}(T)$ dependence appearing for $\text{Bi}_{1.6}\text{Pb}_{0.4}\text{Sr}_2\text{CaCu}_2\text{O}_{8+\delta}$ single crystals.¹⁴ On the other hand, it has been suggested¹⁵ that the minimum in $H_{\text{on}}(T)$ observed for overdoped $\text{Bi}_2\text{Sr}_2\text{CaCu}_2\text{O}_{8+\delta}$ single crystals can be described using the cage model from Ref. 3, originally formulated for the melting of the vortex system in the presence of pinning. In all these attempts, the theoretically predicted transition field (for static conditions) is identified with H_{on} determined in global and/or local magnetic measurements. The shift of the SMP to higher H values with decreasing T in the low- T domain was reported for $R\text{Ba}_2\text{Cu}_3\text{O}_{7-\delta}$ ($R = \text{Y}, \text{Nd}, \text{Yb}$)¹⁶ and $\text{Pb}_2\text{Sr}_2\text{Y}_{0.53}\text{Ca}_{0.47}\text{Cu}_3\text{O}_{8+\delta}$ single crystals,¹⁷ as well.

In this work, we extended the study performed in Ref. 11 for $\text{La}_{2-x}\text{Sr}_x\text{CuO}_4$ single crystals in H parallel to the c axis to lower temperatures, down to $T = 2$ K. It was found that H_{on} increases significantly with decreasing T , even in the low- T region, where all the superconductor parameters are practi-

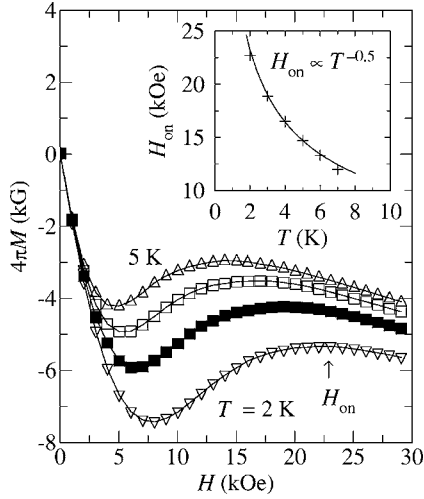


FIG. 1. Main panel: Magnetization curves $M(H)$ of overdoped $\text{La}_{2-x}\text{Sr}_x\text{CuO}_4$ single crystals ($x=0.19$) with the external magnetic field H (oriented along the c axis) around the onset field H_{on} for the second magnetization peak in the low-temperature T range ($T=2, 3, 4,$ and 5 K). As shown in the inset, the $H_{\text{on}}(T)$ dependence at low T approximately takes the form $H_{\text{on}}(T) \propto T^{-0.5}$.

cally independent of T . We show that the upward curvature of the order-disorder transition line determined in standard magnetization measurements at low T is essentially due to the influence of the macroscopic currents induced in the sample.¹¹ A simple energy balance equation for the order-disorder transition at low T in the dynamic conditions specific to the widely used magnetization measurements is proposed.

The magnetization M (identified with the irreversible magnetization) of overdoped $\text{La}_{2-x}\text{Sr}_x\text{CuO}_4$ (LSCO) single crystals (with $x=0.19$) was measured in zero-field cooling conditions and H oriented parallel to the c axis, using a commercial Quantum Design SQUID magnetometer in the RSO mode and/or a magnetometer with extraction. The results obtained in increasing or decreasing H are similar. The relaxation time t was considered to be zero when the magnet charging was finished. LSCO single crystals were grown by the traveling solvent floating zone method.¹⁸ The investigated samples have the zero-field critical temperature $T_c \approx 28$ K, a transition width of ≈ 1.5 K, $\gamma=15-18$, and the normal state resistivity of the order of $1 \text{ m}\Omega \text{ cm}$. The characteristic sample dimensions were $\sim 1 \times 1 \times 0.8 \text{ mm}^3$, with the smallest dimension along the c axis.

LSCO single crystals exhibit a SMP over a large T interval.¹¹ Figure 1 illustrates the magnetization curves $M(H)$ for H around H_{on} and T down to 2 K. The striking feature is that H_{on} has a significant variation with T , even in the low- T domain, where both E_{cl} and E_{pin} are independent of T . As shown in the inset to Fig. 1, the $H_{\text{on}}(T)$ dependence at low T approximately takes the form $H_{\text{on}}(T) \propto T^{-0.5}$.

The time evolution of H_{on} is shown in Fig. 2, where M was registered at $t=t_1=28$ s, $t=t_2=150$ s, and $t=t_3=1200$ s. H_{on} decreases with increasing t , as often reported. In the framework of the energy balance equation, the shift of H_{on} to lower values at high t indicates an increase of the actual pinning energy U_p , and this can be caused by the relaxation

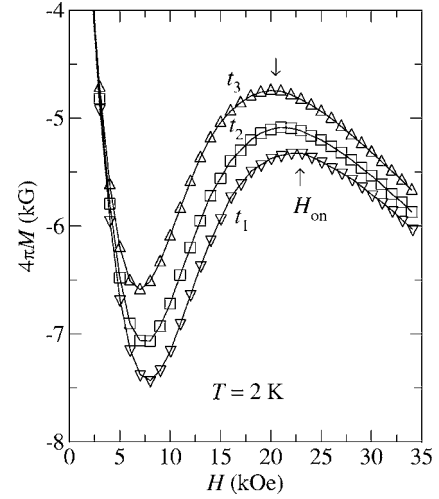


FIG. 2. The time t evolution of the onset field H_{on} at $T=2$ K, where the magnetization M was registered at $t=t_1=28$ s, $t_2=150$ s, and $t_3=1200$ s after H was applied in the hysteresis mode (no overshoot) for $t=t_1$, and with the magnet in the persistent mode at t_2 and t_3 . H_{on} decreases with increasing t , as often reported.

of the macroscopic currents induced in the sample during magnetization measurements. For the dynamic conditions characteristic to standard magnetization measurements, an appropriate energy balance equation at low T and $t=t_1$, for example, would be

$$E_{\text{cl}}(H) = U_p[H, J(t_1)], \quad (1)$$

where $J \propto |M|$ is the current density, and $E_{\text{cl}}(H) \propto H^{-0.5}$.¹⁹ The collective pinning behavior^{19,20} for H around H_{on} generates a nonlinear J variation of the actual pinning energy: $U_p(J) \approx U_c(J_c/J)^\mu$, where U_c is the collective pinning energy, J_c is the critical current density, and $\mu > 0$ is the collective pinning exponent. This is confirmed by the T variation of the first measured magnetization $M(t_1, T)$ plotted in the main panel of Fig. 3, which can be fitted by the collective pinning result,

$$M(t_1, T) \propto J_c [(T/U_c) \ln(t_1/t_0)]^{-1/\mu}, \quad (2)$$

where t_0 is the time scale for creep.¹⁹ Neglecting the T variation of J_c , U_c , and of $\ln(t_0)$ in the considered T interval, the two-parameter fit of the data in the main panel of Fig. 3 with Eq. (2) gives $\mu \approx 1$.

In our approach, $U_p(J)$ at low T is substituted by the actual activation energy $U(J)$ in the classic vortex creep process. Using magnetization relaxation data for a short time interval (≈ 100 s) in the vicinity of t_1 , where $M(t)$ in double logarithmic scales can be approximated by a straight line, as illustrated in the inset to Fig. 3, we determined the normalized vortex creep activation energy $U^* = -T\Delta \ln(t) / \Delta \ln(|M|)$. From the general vortex-creep relation,²¹ $U(J) = T \ln(t)$, and $J \propto |M|$, one obtains $U^*(J) = \mu U_p(J)$, and, for $t=t_1$, the energy balance equation at low T becomes

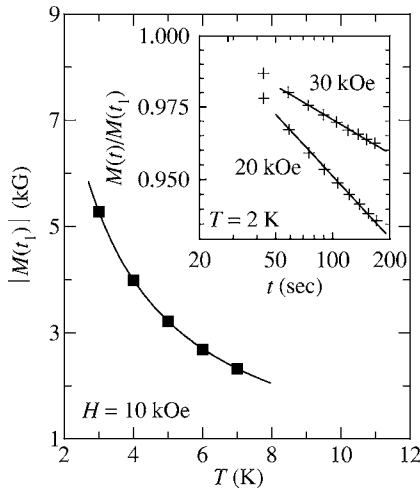


FIG. 3. Main panel: Temperature T variation of the first measured magnetization $M(t_1, T)$ (where $t_1=28$ s) for $H=10$ kOe, fitted by the collective pinning result [Eq. (2)]. Inset: Magnetization relaxation $M(t)$ normalized to $M(t_1)$ at $T=2$ K and $H=20$ and 30 kOe. For a short time interval close to t_1 , a straight line can approximately fit the data in double logarithmic scales.

$$E_{\text{el}}(H) = (\alpha/\mu)U^*(T, H), \quad (3)$$

where $\alpha \approx \text{constant}$, and $U^*(T)$ appears, owing to the T variation of the $J(t_1)$. The applicability of Eq. (3) in the case of standard magnetization measurements at low T [where $U^*(J)$ does not essentially involve intervortex interactions¹⁹] is supported by the determined $U^*(T)$ for H around H_{on} and $U^*(H)$ for H just above H_{on} , as shown below.

The $U^*(H)$ dependence for $H=10$ kOe is plotted in the main panel of Fig. 4. The linear increase of U^* with increasing T in the low- T range²² is a result of the relatively strong $U^*(J)$ variation in the collective pinning regime and the usually fixed relaxation time window in standard magnetization measurements, as discussed in Ref. 17.

The $U^*(H)$ variation for H just above H_{on} at $T=2$ K is shown in the inset to Fig. 4, and a two-parameter fit of the data gives $U^*(H) \propto H^{1.45}$. The $U^*(H)$ increase is in qualitative agreement with the collective pinning behavior observed between H_{on} and the peak field at low relaxation levels.²³ However, it also reflects the coexistence of the Bragg glass and the disordered vortex phase in the sample for H between H_{on} and the peak field.

With Eq. (3), where $\alpha, \mu = \text{const}$, $U^*(T)$ and $U^*(H)$ in the low- T range from Fig. 4 lead to $H_{\text{on}}(T) \propto T^{-0.51}$, which is very

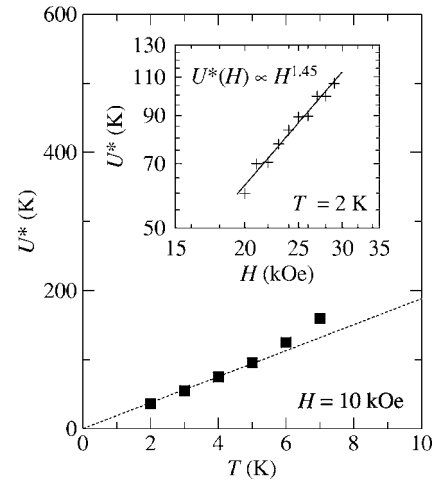


FIG. 4. T dependence (main panel) and the H variation (inset) of the normalized vortex creep activation energy $U^* = -T\Delta \ln(t)/\Delta \ln(|M|)$ determined using the short time magnetization relaxation $M(t)$ data, as illustrated in the inset to Fig. 3. For H around H_{on} , U^* decreases linearly with decreasing T in the low- T range, whereas $U^*(H)$ and $T=2$ K and H just above H_{on} is approximately of the form $U^*(H) \propto H^{1.45}$.

close to that experimentally observed (see the inset to Fig. 1).

Thus, the location of the $H_{\text{on}}(T)$ boundary determined in standard magnetization measurements at low T is highly influenced by the macroscopic currents induced in the sample. With decreasing T in the low- T range, the induced current density $J(t_1)$ increases toward J_c , since the overall relaxation in the time interval from t_0 to t_1 diminishes. This is similar to the increase of the current density in a transport measurement, and the related reduction of the effective pinning generates the (dynamic) ordering of the vortex system.^{24–27} When the influence of nonuniform surface barriers²⁸ is small, the dynamic ordering of the vortex system during magnetization measurements at low T appears in $\text{Bi}_2\text{Sr}_2\text{CaCu}_2\text{O}_{8+\delta}$ single crystals, as well. In this case, the limitation of the $H_{\text{on}}(T)$ increase with decreasing T by the crossover field¹⁹ $B_{2D} \approx \Phi_0/\gamma^2 s^2$ (where s is the distance between the Cu-O layers) leads to the disappearance of the SMP at low T .²⁹

This work has been supported by the Japan Society for the Promotion of Science, and by EC through the Human Potential Program under Contract No. HPRI-1999-CT-00030. We thank T. Sasagawa, for providing us with LSCO samples.

¹T. Giamarchi and P. Le Doussal, Phys. Rev. B **52**, 1242 (1995); **55**, 6577 (1997).

²V. Vinokur, B. Khaykovich, E. Zeldov, M. Konczykowski, R. A. Doyle, and P. Kes, Physica C **295**, 209 (1998).

³D. Ertaş and D. R. Nelson, Physica C **272**, 79 (1996).

⁴G. P. Mikitik and E. H. Brandt, Phys. Rev. B **64**, 184514 (2001).

⁵V. N. Kopylov, A. E. Koshelev, I. F. Schegolev, and T. G. Togonidze, Physica C **223**, 291 (1990).

⁶M. Daeumling, J. M. Seuntjens, and D. C. Larbalestier, Nature (London) **346**, 332 (1990).

⁷B. Khaykovich, E. Zeldov, D. Majer, T. W. Li, P. H. Kes, and M. Konczykowski, Phys. Rev. Lett. **76**, 2555 (1996).

- ⁸D. Giller, A. Shaulov, Y. Yeshurun, and J. Giapintzakis, *Phys. Rev. B* **60**, 106 (1999).
- ⁹T. Nattermann, *Phys. Rev. Lett.* **64**, 2454 (1990).
- ¹⁰J. Kierfeld and V. Vinokur, *Phys. Rev. B* **61**, R14928 (2000).
- ¹¹Y. Radzyner, A. Shaulov, Y. Yeshurun, I. Felner, K. Kishio, and J. Shimoyama, *Phys. Rev. B* **65**, 214525 (2002).
- ¹²Y. Radzyner, A. Shaulov, and Y. Yeshurun, *Phys. Rev. B* **65**, 100513(R) (2002).
- ¹³G. P. Mikitik and E. H. Brandt, *Phys. Rev. B* **68**, 054509 (2003).
- ¹⁴M. Baziljevich, D. Giller, M. McElfresh, Y. Abulafia, Y. Radzyner, J. Schneck, T. H. Johansen, and Y. Yeshurun, *Phys. Rev. B* **62**, 4058 (2000).
- ¹⁵D. Darminto and M. O. Tjia, *Physica C* **412–414**, 472 (2004).
- ¹⁶M. Werner, F. M. Sauerzopf, H. W. Weber, and A. Wisniewski, *Phys. Rev. B* **61**, 14795 (2000).
- ¹⁷L. Miu, S. Popa, T. Noji, Y. Koike, D. Miu, S. Diaz, and G. Chouteau, *Phys. Rev. B* **70**, 134523 (2004).
- ¹⁸T. Sasagawa, Y. Togawa, J. Shimoyama, A. Kapitulnik, K. Kitazawa, and K. Kishio, *Phys. Rev. B* **61**, 1610 (2000).
- ¹⁹G. Blatter, M. V. Feigel'man, V. B. Geshkenbein, A. I. Larkin, and V. M. Vinokur, *Rev. Mod. Phys.* **66**, 1125 (1994).
- ²⁰M. V. Feigel'man, V. B. Geshkenbein, A. I. Larkin, and V. M. Vinokur, *Phys. Rev. Lett.* **63**, 2303 (1989).
- ²¹V. B. Geshkenbein and A. I. Larkin, *Sov. Phys. JETP* **60**, 639 (1989).
- ²²Y. Xu, M. Suenaga, A. R. Moodenbaugh, and D. O. Welch, *Phys. Rev. B* **40**, 10882 (1989).
- ²³L. Miu, T. Noji, Y. Koike, E. Cimpoiasu, T. Stein, and C. C. Almasan, *Phys. Rev. B* **62**, 15172 (2000).
- ²⁴S. Bhattacharya and M. J. Higgins, *Phys. Rev. Lett.* **70**, 2617 (1993).
- ²⁵A. B. Kolton, D. Domínguez, C. J. Olson, and N. Grønbech-Jensen, *Phys. Rev. B* **62**, R14657 (2000).
- ²⁶C. J. Olson, C. Reichhardt, and V. M. Vinokur, *Phys. Rev. B* **64**, 140502(R) (2001).
- ²⁷U. Yaron, P. L. Gammel, D. A. Huse, R. N. Kleiman, C. S. Oglesby, E. Bucher, B. Batlogg, D. J. Bishop, K. Mortensen, and K. N. Calusen, *Nature (London)* **376**, 753 (1995).
- ²⁸B. Kalisky, D. Giller, A. Shaulov, and Y. Yeshurun, *Phys. Rev. B* **67**, 140508(R) (2003).
- ²⁹L. Miu, *Physica C* **405**, 260 (2004).